Shower power: isolating the prompt atmospheric neutrino flux using electron neutrinos

John F Beacom[1,2,3] and Julián Candia[4,5]

[1] Department of Physics, The Ohio State University, Columbus, OH 43210, USA
[2] Department of Astronomy, The Ohio State University, Columbus, OH 43210, USA
[3] NASA/Fermilab Astrophysics Center, Fermi National Accelerator Laboratory, Batavia, IL 60510-0500, USA
[4] IFLP/Departamento de Física, Universidad Nacional de La Plata, CC 67, La Plata 1900, Argentina
[5] Theoretical Physics Department, Fermi National Accelerator Laboratory, Batavia, IL 60510-0500, USA
E-mail: beacom@mps.ohio-state.edu and candia@fisica.unlp.edu.ar

Abstract. At high energies, the very steep decrease of the conventional atmospheric component of the neutrino spectrum should allow the emergence of even small and isotropic components of the total spectrum, indicative of new physics, provided that they are less steeply decreasing, as generically expected. One candidate is the prompt atmospheric neutrino flux, a probe of cosmic ray composition in the region of the knee as well as small-x QCD, below the reach of collider experiments. A second is the diffuse extragalactic background due to distant and unresolved AGNs and GRBs, a key test of the nature of the highest-energy sources in the universe. Separating these new physics components from the conventional atmospheric neutrino flux, as well as from each other, will be very challenging. We show that the charged-current *electron* neutrino 'shower' channel should be particularly effective for isolating the prompt atmospheric neutrino flux, and that it is more generally an important complement to the usually considered charged-current *muon* neutrino 'track' channel. These conclusions remain true even for the low prompt atmospheric neutrino flux predicted in a realistic cosmic

ray scenario with heavy and varying composition across the knee (Candia and Roulet, 2003 *J. Cosmol. Astropart. Phys.* JCAP09(2003)005). We also improve the corresponding calculation of the neutrino flux induced by cosmic ray collisions with the interstellar medium.

Keywords: cosmic rays, ultra high energy photons and neutrinos, neutrino detectors, neutrino and gamma astronomy

Contents

1. Introduction

The measured flux of cosmic rays (CRs) at energies up to about 10^{20} eV reveals the existence of powerful accelerators (or perhaps decaying supermassive particles), about which very little else is known for certain [1]. Since the directions of cosmic rays can be scrambled in intervening magnetic fields, point source cosmic ray astronomy could be difficult to achieve [2]–[4]. The same high energy sources may also make gamma rays, which are directional, but which will be absorbed at high energies and large distances by the reaction $\gamma\gamma \to e^+e^-$ on the cosmic infrared background (e.g., near 10^4 GeV the mean free path is about 100 Mpc [5, 6]). In many models of high energy sources, neutrinos are also copiously produced. They have the advantages of being neither deflected nor absorbed even when travelling vast distances, and additionally of being able to escape even from within dense sources. The obvious disadvantage is that they are correspondingly hard to detect, due to their only having weak interactions.

However, for the first time, neutrino telescopes in operation or under construction will have the required sensitivity to test realistic models of the highest energy sources in the universe [7]–[11]. For example, for several nearby active galactic nuclei (AGNs), high energy gamma rays, up to about 10^4 GeV, have been detected [12]–[15]. If these gamma rays arise from neutral pion decays ($\pi^0 \to \gamma\gamma$), then similar fluxes of neutrinos from charged pion decays (e.g., $\pi^+ \to \mu^+\nu_\mu$) are expected. The pions are naturally produced in models in which a high energy proton flux collides in the source with either other nucleons or photons in the ambient radiation field. The AMANDA detector is beginning to test these models at a level competitive with gamma ray telescopes [16]–[22].

Besides point sources, neutrino telescopes can also measure the diffuse background arising from more distant and higher energy sources, those which would not be directly visible with gamma rays, due to the opacity of the cosmic infrared background. However, it will be quite challenging to distinguish a diffuse extragalactic background from the very large flux of neutrinos produced by cosmic ray collisions with Earth's atmosphere. The atmospheric neutrino spectrum falls as $E^{-\gamma}$, with the spectral index in the range $\gamma \simeq 3\text{–}3.7$. Due to relativistic time dilation effects, the higher the energy of the mesons produced in the atmosphere, the larger the amount of energy lost during their propagation before they decay. Hence, the atmospheric neutrino flux has a spectral index similar to the CR spectrum at lower energies (i.e. $\gamma \simeq 3$), while it becomes steeper at higher energies. Since the expected extragalactic spectrum is harder (indeed, it is thought to fall as E^{-2}), a non-atmospheric component could be discovered as a break in the spectrum. Below the break the spectrum would be background dominated, and above the break signal dominated. However, initially the statistics above the break would be poor, both by definition of a first discovery, and because the spectra are steeply falling.

The atmospheric neutrinos have been well measured at low energies by Super-Kamiokande and other detectors [23, 24], and now have also been detected at higher energies by AMANDA [25]. The flux seen so far is the 'conventional' atmospheric flux, arising from pion and kaon decays, and it is reasonably well understood in terms of the cosmic ray spectrum and composition, meson production cross sections, and meson propagation and decay in the atmosphere. Indeed, the uncertainty for the absolute flux of the low energy atmospheric neutrinos is in the range 10–20% [7, 24]. At higher energies, neutrino fluxes from very short lived hadrons dominate, and the 'prompt' atmospheric neutrino flux is much less understood; empirically, so far not at all. For these predictions, there are significant uncertainties due to both the cosmic ray composition as well as small-x QCD (beyond the reach of colliders); these issues are discussed in detail below.

So if and when neutrino telescopes first claim discovery of an extragalactic neutrino flux by a break in the spectrum, the question will of course arise of whether the effect is real, or just a fluctuation. In this respect, different detection channels would be invaluable. If the signal is real, it could be an important signature of new physics, in one of two ways: (i) as the prompt atmospheric neutrino flux, and hence a new probe of both cosmic rays and QCD, or (ii) as a real extragalactic flux, and hence a new probe of the high energy universe. Distinguishing these possibilities also requires different detection channels.

The main focus in neutrino telescope studies has been the ν_μ charged-current detection channel, to be measured with upward throughgoing muons. Since by a few hundred GeV the muon range in ice exceeds 1 km, the effective detection volume is no longer the detector volume, but rather the detector area times the muon range, which increases with energy. This effect, combined with the rising neutrino cross section, partially ameliorates the effect of the steeply falling neutrino spectra.

We propose a new method for isolating the prompt atmospheric neutrino flux, which, as described above, is important both in its own right, and as a background to extragalactic fluxes. Our proposed method focuses on the channel of ν_e charged-current events, stressing the importance of considering the event spectrum as a function of *detectable* energy, and not simply as the product of flux and cross section as a function of the *neutrino* energy. Although several analyses based on shower events have already been performed (for instance, using BAIKAL [26]–[28] and AMANDA [19]–[21] data), this channel has received

Table 1. Brief summary of the distinguishing signatures of the relevant neutrino flux components. For the different energy spectra, see the figures.

Neutrino flux	Flavours (ν_e:ν_μ:ν_τ)	Angular dependence
Conventional atmospheric	$\frac{1}{20}$:1:0	Peaks at horizon
Prompt atmospheric	1:1:$\frac{1}{10}$	Isotropic
Galactic	1:1:1	Peaks at Galactic centre
Extragalactic	1:1:1	Isotropic; point/transient sources

little attention in the theoretical literature [29]–[40]. However, here we point out that it has several advantages over the usually considered ν_μ charged-current detection channel. For either the prompt atmospheric or extragalactic fluxes, the ν_e fraction is large, whereas it is small for the conventional atmospheric flux at high energies. We will show that in this channel the spectral break occurs about an order of magnitude lower in energy than in the ν_μ channel; this is an advantage because at lower energies the fluxes are higher and Earth absorption effects are less. Several authors have focused on the detection of ν_τ; however, at energies below about 5×10^6 GeV it is challenging to separate individual ν_τ interactions from those of other flavours. The ν_e channel should be particularly effective for prompt atmospheric neutrinos, since their spectrum falls more steeply than the extragalactic spectrum, and hence benefits more from a lower threshold. Moreover, there is much better spectral fidelity between neutrino energy and detected energy than in ν_μ charged-current interactions, which is important when searching for a spectral break. It should also be noticed that the intrinsic experimental resolutions of under-ice/water detectors are better for shower events. Indeed, the detector response can be better calibrated by means of *in situ* light sources, and the calorimetric measurement is easier for a shower than for a muon track, since in the former the energy is deposited within a small region.

Below, we present our results in more detail, reviewing the various fluxes and their characteristics, and how this picture is made more realistic and in fact more encouraging by considering the *detectable* spectra. We focus on a realistic prediction for the prompt atmospheric neutrino flux that takes into account the heavy and varying cosmic ray composition in the region of the knee [37]. This model also has important implications for the diffuse neutrinos from the Galactic centre, and we present an improved calculation of this flux. We also show how the prompt atmospheric neutrino flux changes with different assumptions about the cosmic ray composition. Finally, we summarize our main results.

2. Calculations and results

2.1. Neutrino fluxes

In figure 1, we display the main components of the high energy neutrino flux, and how their relative importance changes across the spectrum. In table 1, we list other identifying characteristics of these components, of which the neutrino flavour ratios are particularly important.

At low energies, the flux is dominated by conventional atmospheric neutrinos, which arise from the decays of charged pions and kaons produced by cosmic rays hitting the top
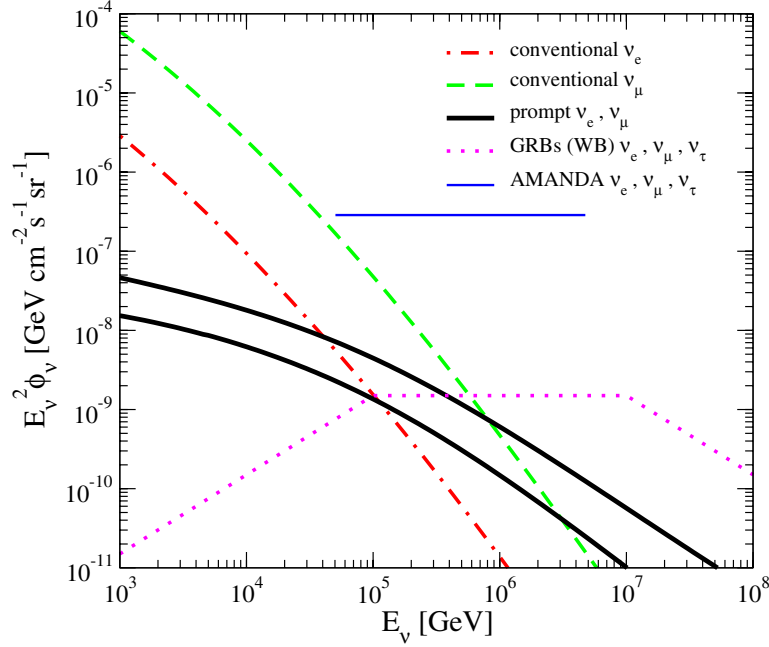
Figure 1. The major components of the high energy neutrino spectrum are shown, along with labels indicating their flavour content. Here and throughout, fluxes are given per flavour (but adding neutrinos and antineutrinos). For the atmospheric neutrinos, we consider the heavy and varying cosmic ray composition scenario of Candia and Roulet [37]; the conventional atmospheric neutrino flux has been averaged over the zenith angle. The two curves for the prompt atmospheric neutrino flux indicate the adopted range of small-x QCD uncertainties. As an example of a low diffuse extragalactic flux, the Waxman–Bahcall prediction for GRBs is shown [41]. On the high side, any extragalactic or prompt atmospheric neutrino flux is subject to the latest AMANDA bound [21].

of the atmosphere [42]–[54]. Although the pion flux is larger than the kaon flux, above a few hundred GeV, the pions are more likely to interact before decaying, and due to this the kaon contribution to the neutrino flux dominates at high energies. Unlike pions, kaons do decay to electron neutrinos with an appreciable branching ratio, about 5%. However, this is small enough to serve as a key part of our argument. Note that tau neutrinos arise in the conventional atmospheric neutrino flux only via neutrino oscillations (very suppressed at high energies), and hence are ignored here (see figure 7 of [36] for an illustration).

Above about 10^3 GeV, kaons are also significantly attenuated before decaying, and the prompt component, arising mainly from the decay of short lived charmed mesons $D^{\pm}, D^0, D_s$ and Λ_c, becomes increasingly important [29]–[40]. In these decays, the branching ratios for electron and muon neutrinos are nearly equal, which is also a key point. The prompt tau neutrino flux is about ten times smaller, and is ignored here. In figure 7 of [36], it is shown that the prompt tau neutrino flux dominates the conventional tau neutrino flux, even above relatively low energies. However, it is challenging to individually identify tau neutrino events in detection until energies of about 5×10^6 GeV;

due to their different propagation in Earth, it may be possible to recognize their presence in a statistical sense at lower energies [55]–[62].

The evaluation of the prompt neutrino flux requires taking into account next to leading order processes in the charm production cross section, which strongly depend on the behaviour of the parton distribution functions at small x, below the lowest values ($x \sim 10^{-5}$) probed in collider experiments. Hence, depending on how the parton distribution functions are extrapolated, the results appear to spread over more than an order of magnitude. In order to illustrate this uncertainty range, figure 1 shows results obtained using two different structure distribution functions, namely the CTEQ3 parton distribution function [32, 63] and the Golec-Biernat, Wüsthoff (GBW) model [36, 40, 64, 65], which includes gluon saturation effects.

The prompt atmospheric neutrino flux also strongly depends on the assumed composition of the cosmic rays. Let $\phi_Z = \phi_{0Z} E^{-\gamma_Z}$ be the CR spectrum associated with the CR component of nuclei of charge Z and average mass A, where the spectral index is typically $\gamma_Z \simeq 2.7$ below the knee, and generally larger above it. This nuclear component provides a nucleon spectrum $\phi_{N,Z}(E_N) = A^2 \phi_Z(E = AE_N)$, which hence corresponds to a contribution suppressed by a factor $A^{2-\gamma_Z}$ in the fluxes. Thus, for the same spectrum, a heavier composition results in a lower CR nucleon flux, and hence corresponds to lower neutrino fluxes. Following Candia and Roulet [37], a mixed composition of cosmic rays with all different nuclear species ranging from hydrogen to nickel was considered. While the detailed composition of the different nuclear components below the knee is well known from experimental observations, at higher energies a rigidity dependent scenario is assumed, in which each cosmic ray component changes its spectral index by $\Delta\gamma \simeq 2/3$ across the knee, as can arise, e.g., in the so-called diffusion/drift scenario [66, 67]. Below we will discuss the effects of varying the cosmic ray composition. In figure 1, we show both the conventional and prompt atmospheric neutrino fluxes predicted in this realistic mixed-composition model of cosmic rays. While the prompt atmospheric neutrinos are isotropic, the conventional atmospheric neutrinos peak at the horizon; in our calculations, we present the conventional fluxes averaged over the upper hemisphere.

In figure 1, we also show the latest AMANDA limit on the high energy neutrino flux, obtained from their shower analysis [20, 21]. The single-flavour AMANDA bound shown in the figure was obtained neglecting single-flavour detection efficiencies, and simply dividing by three for assumed equal flavour ratios. Indeed, this bound, which should be regarded as an estimate for the upper limit of a single-flavour neutrino flux, is also consistent with the results of the BAIKAL experiment [26]–[28]. It should be noted that past predictions of the prompt atmospheric neutrino flux were larger by up to a few orders of magnitude beyond what we consider here. While probably not realistic, even a very large flux would be consistent with the present AMANDA bound. We focus on the difficult but realistic case of a small prompt flux. We also assume a small extragalactic flux (for illustration, the Waxman and Bahcall gamma-ray burst (GRB) model [22, 41]); for a generic astrophysical neutrino source, one expects a ratio of neutrino fluxes at production of 1:2:0, transformed by neutrino oscillations en route into 1:1:1 (though new physics in the neutrino sector could alter both the fluxes and the flavour ratios [58], [68]–[72]). If the actual fluxes are larger than assumed here, then our proposed technique will be easier to use.

2.2. Detected spectra

Figure 1 shows that the prompt atmospheric and the extragalactic neutrino spectra might not emerge from the much larger conventional atmospheric neutrino spectrum until energies as large as 10^6 GeV. To be precise, this is only true for the ν_μ spectrum, and the corresponding charged-current channel based on the detection of long-ranging muon tracks. If the ν_e spectrum could be isolated, then the spectral break could occur an order of magnitude lower in energy, where the fluxes are much larger (and note that figure 1 shows $E^2\, \mathrm{d}N/\mathrm{d}E$, not the spectra themselves). Our strategy is therefore to reduce the conventional atmospheric neutrino background by *excluding* charged-current ν_μ events with muon tracks, and concentrate on ν_e charged-current events, which initiate showers (also known as cascades). As shown in figure 1 and table 1, the signals all have equally large ν_e and ν_μ fluxes, while the background due to conventional atmospheric neutrinos has a low ν_e content. While conventional atmospheric ν_μ will contribute to the shower rate via their neutral-current interactions, their importance is greatly reduced.

In a neutrino interaction with a nucleon, the neutrino energy E_ν is shared between the outgoing quark, given a fraction y, and the outgoing lepton, given a fraction $1 - y$. The differential cross sections for charged- and neutral-current interactions both peak at $y = 0$. In a charged-current ν_e interaction, the quark initiates a hadronic shower of energy $\simeq yE_\nu$, and the electron an electromagnetic shower of energy $\simeq(1 - y)E_\nu$, so that the total visible energy $E_{\mathrm{vis}} \simeq E_\nu$. We assume that hadronic and electromagnetic showers are indistinguishable in the detector. In a neutral-current interaction, E_{vis} is thus smaller by a factor $\langle y \rangle \simeq 0.4$–$0.3$ (falling with increasing energy) [73]. Further, neutral-current total cross sections are smaller than the charged-current cross sections, $\sigma_{\mathrm{NC}}/\sigma_{\mathrm{CC}} \simeq 0.4$ [73]. Taking into account that the conventional atmospheric neutrino spectrum is very steeply falling (with a spectral index in the range $\gamma \simeq 3$–3.7, as mentioned above), it turns out that the ν_μ shower fluxes arising from neutral-current interactions are suppressed by a factor $\sim \langle y \rangle^{(\gamma-1)} \times \sigma_{\mathrm{NC}}/\sigma_{\mathrm{CC}}$, i.e. roughly an order of magnitude relative to the shower fluxes arising via ν_e charged-current interactions.

Thus in the detected spectrum of showers from conventional atmospheric neutrinos, the contributions from ν_e and ν_μ are comparable, the difference in flux (see figure 1) being compensated by the difference in detectability. Our results for the conventional atmospheric neutrinos are shown in figure 2. As noted, we are excluding ν_μ charged-current events, which can be recognized by the presence of long-ranging muon tracks. The spectra shown in the figure were calculated by convolving the assumed neutrino spectra with the differential cross section (averaged between neutrinos and antineutrinos) [73]. Figure 2 shows that the techniques described here can greatly reduce the background due to conventional atmospheric neutrinos.

Since the prompt atmospheric and the extragalactic neutrinos have equal ν_e and ν_μ fluxes, the corresponding shower rates will be dominated by ν_e charged-current interactions. Though we include the neutral-current interactions of all relevant flavours, they could be ignored (e.g., compare the relative ν_e charged- and neutral-current rates in figure 2). So far, we have not mentioned the interactions of ν_τ, should they appear in the flux (see table 1). Below about $E_\nu \simeq 5 \times 10^6$ GeV, their charged-current interactions will produce only showers (with $E_{\mathrm{vis}} \simeq E_\nu$), due to the short lifetime of the tau lepton. Above that energy, the length of the tau lepton track becomes long enough that it could be
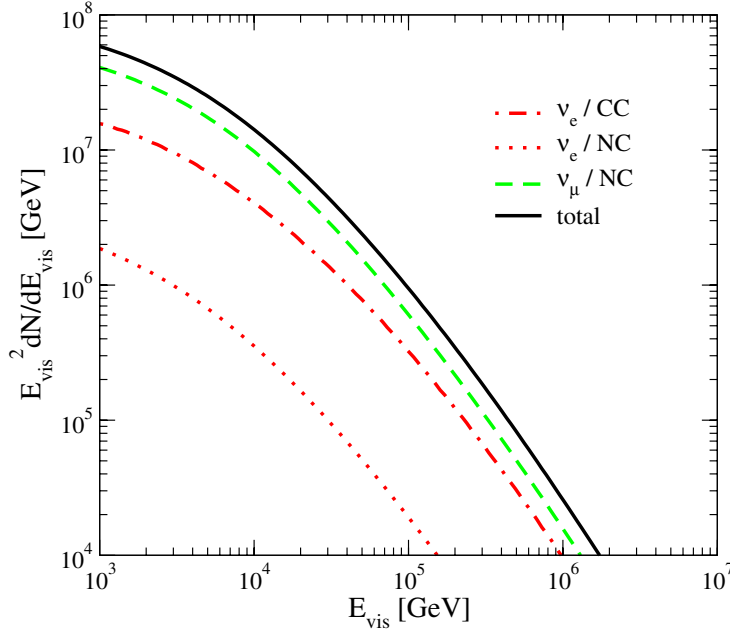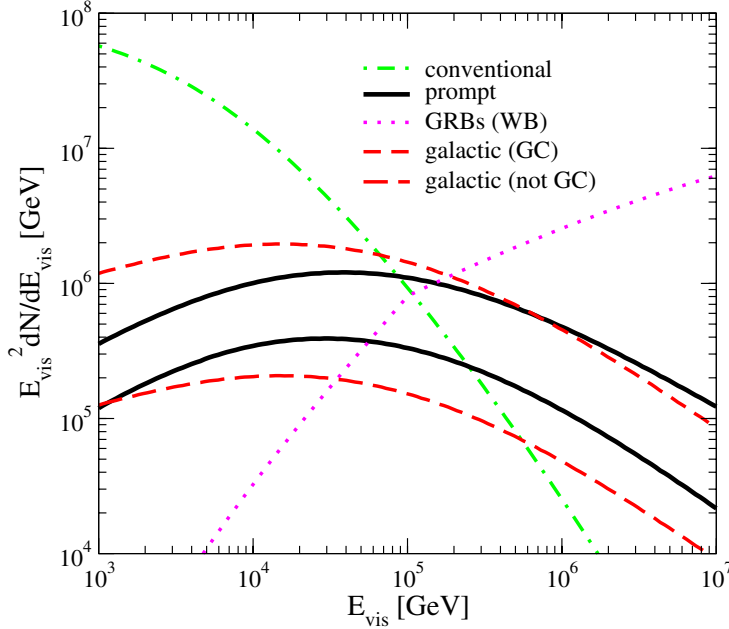
Figure 2. Differential shower rates as a function of visible energy E_{vis}, expected for a km^3 detector after 10 years of data taking, using only downgoing neutrinos, and the fluxes shown in figure 1. Only the components of the conventional atmospheric neutrino spectrum are shown here, with charged-current (CC) and neutral-current (NC) interactions separated for illustration. The relative importance of the ν_{e} CC channel grows with respect to the ν_{μ} NC channel due to the decreasing value of $\langle y \rangle$.

separated from the shower. In the conservative fluxes used in this paper, there is very little flux at such high energies, and we do not consider the separation of those events. When ν_{τ} is present in the flux, we do include their charged- and neutral-current contributions to the detected shower spectrum. However, we do note that since the ν_{τ} fraction in the prompt atmospheric neutrino flux is small, the direct identification of any ν_{τ} candidates would strongly indicate an extragalactic origin. A more detailed description of the characteristics of the different kinds of events in a neutrino telescope, and their relative detectability, is given in [58].

Figure 3 shows the *detectable* shower spectra corresponding to figure 1. The energy at which the prompt atmospheric or extragalactic signals might emerge from the background of the conventional atmospheric neutrinos is now an order of magnitude lower. Had we only presented the flux or the flux times total cross section versus *neutrino* energy, this important fact would not have been evident. Hooper *et al* [39] also proposed determination of the prompt atmospheric and the extragalactic neutrino spectra by means of the shower spectra. However, there are key differences between our calculation and theirs. We assume that all ν_{μ} charged-current events can be excluded by recognizing their long-ranging muon tracks; they included ν_{μ} charged-current interactions in the detector volume, even though they state that it would be better to exclude them. More importantly, we expressed the spectra as a function of *visible*, not *neutrino* energy, which has a very significant effect on

Figure 3. Differential shower spectra as a function of visible energy E_{vis}, expected for a km^3 detector after 10 years of data taking, using only downgoing neutrinos, and the spectra shown in figure 1. As explained, we have used a low prompt atmospheric neutrino flux, corresponding to the realistic cosmic ray composition model; the AMANDA bound [21] would allow it to be about two orders of magnitude larger. The spectra from neutrinos produced by cosmic ray collisions in the galaxy are also shown with long-dashed curves, with their normalization explained in the text.

reducing the background from conventional atmospheric neutrinos. Taking these effects into account allows us to realistically consider much smaller prompt atmospheric and also extragalactic fluxes than Hooper *et al* [39].

The shower channel does not provide specific information on the neutrino flavour, and it cannot distinguish charged- and neutral-current events, but this is not a significant disadvantage, and is more than overcome by the much better fidelity between neutrino and visible energy, which is essential for resolving a break in the energy spectrum. The angular resolution is only moderate ($\simeq 20°$, compared to $\simeq 1°$ for the ν_μ charged-current channel), but this is perfectly adequate for an isotropic flux.

One of the disadvantages of the shower detection channel is that atmospheric muons can produce a significant background if they pass near the detector and initiate a shower via a hard bremsstrahlung event. Indeed, the current AMANDA shower limit is set completely by this background [20, 21]. However, since this is a surface effect, the much larger size of IceCube should allow reduction of this background while maintaining a large enough fiducial volume. A similar cut on the outer region of the detector will also be necessary to cut ν_μ charged-current events in which the shower registers in the detector but the muon track escapes. In fact, besides the case in which the muon does not emerge from the region of the shower, the experimental rejection of ν_μ charged-current events also depends on the efficient experimental identification of the muon track, which might

be relatively dim in comparison to the bright hadronic shower. These cuts will reduce the exposure from what we have assumed. However, it has to be noticed that, in order to avoid the effects of absorption in Earth, we have considered only downgoing neutrinos. Neutrinos passing through the whole diameter of Earth are absorbed at about 4×10^4 GeV while, for shorter distances, the absorption energy is significantly higher (e.g., see figure 2 of [74]). Thus the exposure in the relevant energy range could be increased from what we assumed by using also a large fraction of the upgoing events. Even though it strongly peaks at the horizon, we have averaged the conventional atmospheric neutrino flux over the whole upper hemisphere. A more careful treatment of this background, cutting events near the horizon, would allow the signals to be seen at lower energies than shown in our figures. Finally, as we have stressed, the prompt atmospheric neutrino flux considered here is low compared to other models in the literature [29]–[40], as well as to the current AMANDA limit [21], so there is quite a bit of room for straightforward improvement of the limit. A full treatment of the sensitivity and the ability to separate the flux components, using the Monte Carlo techniques developed by Kowalski [20], would be very interesting.

2.3. Diffuse Galactic flux

So far, we have discussed the neutrino fluxes produced either in the atmosphere or extragalactic sources, but have omitted the diffuse Galactic flux that arises mainly from pion and muon decays following cosmic ray interactions with the interstellar medium [75]–[79] (we neglect the possible neutrino flux from a point source at the Galactic centre). In fact, the diffuse Galactic neutrino flux can be comparable to the other high energy components [37]. Since the Galactic flux is expected to be linear in the column depth traversed through the interstellar medium, it is peaked in the direction of the Galactic centre, hence showing an anisotropy in Galactic coordinates. In [76], the matter density of the interstellar medium is given as a function of Galactic coordinates, and a minimum matter density $n = 0.087$ cm^{-3} is assumed. If the Galactic halo is filled with this non-negligible matter density, then the anisotropies in the column density can be ignored except in the direction of the Galactic centre. Assuming a halo with a radius of 20 kpc and a vertical scale height of 2 kpc, the column density in a typical direction is $x_{\text{not-GC}} \simeq 10^{21}$ cm^{-2}; whereas towards the Galactic centre $x_{\text{GC}} \simeq 10^{22}$ cm^{-2}. Previously, the Galactic neutrino flux has been estimated in [37] using $n = 1$ cm^{-3} as a representative mean value for the interstellar matter density in the Galaxy, disregarding the detailed dependence of the matter density as a function of Galactic coordinates. However, given the large uncertainties in the matter distribution in the Galaxy, the estimates of [37] for the column density in the directions orthogonal and parallel to the Galactic plane are in reasonable agreement with the results obtained here.

We separately consider the contribution from the Galactic centre region ($|b| \leq 10°$ and $|l| \leq 10°$, corresponding to a solid angle $\Delta\Omega_{\text{GC}} = 0.12$ sr) and the averaged contribution from all other directions in the upper hemisphere (hence corresponding to $\Delta\Omega_{\text{not-GC}} = 6.16$ sr). This separation is approximately consistent with the angular resolution expected for showers in IceCube.

The differential shower rates for the Galactic components are shown in figure 3, compared to the fluxes discussed already. For directions away from the Galactic centre, the Galactic flux can be neglected compared to the other components of the spectrum. In the
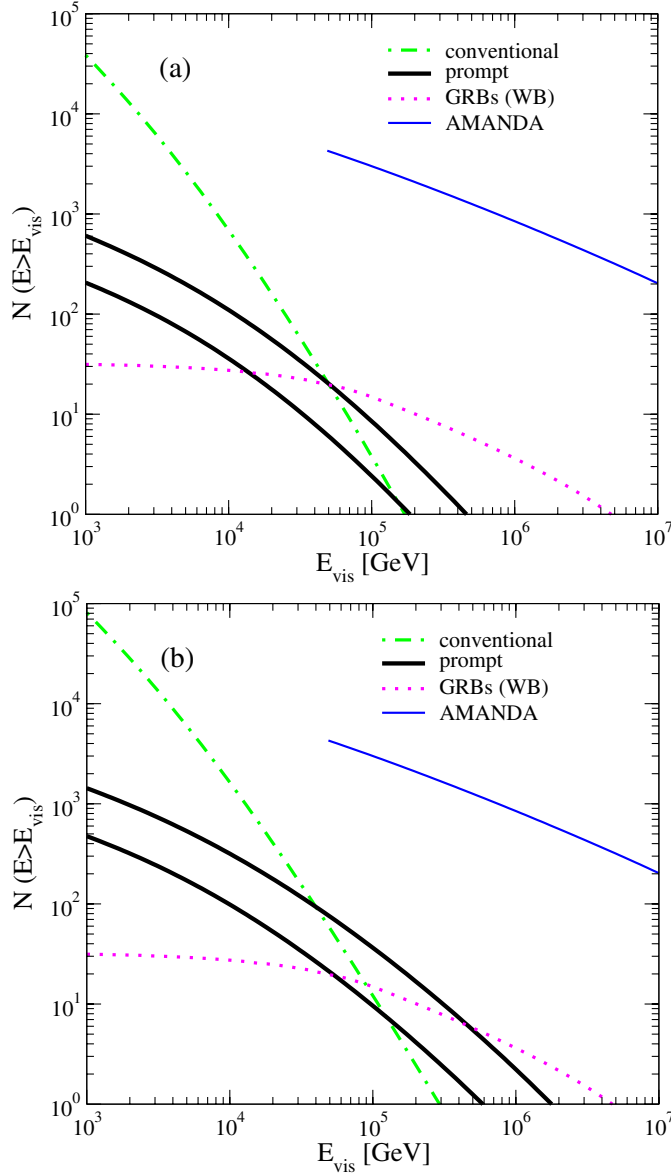
Figure 4. Integral shower rates as a function of visible energy $E_{\rm vis}$, following figure 3. In panel (a), the cosmic ray spectrum has the heavy and varying composition of [37]; in panel (b), the cosmic ray spectrum is assumed to consist only of protons. The line marked 'AMANDA' indicates the resulting integral spectrum assuming an E^{-2} power law, with no upper cut-off, normalized by the AMANDA differential limit [21] (which is actually given over a slightly smaller energy range).

direction of the Galactic centre, the Galactic flux is comparable to the other components. However, in figure 3, we have shown the Galactic centre flux as if it were isotropic. To calculate the true event rates from the Galactic centre direction, this and the other fluxes must be reduced by the small angular acceptance, $\Delta\Omega_{\rm GC}/\Delta\Omega_{\rm not\text{-}GC} \simeq 0.02$, making them too small to be detectable.

2.4. Effects of cosmic ray composition

Figures 4(a) and (b) show the integral shower rates corresponding to the relevant components of the total high energy neutrino spectrum. In figure 4(a), it is assumed that all nuclear species in the range $1 \leq Z \leq 28$ contribute to the composition in a rigidity dependent scenario for the CR knee [37, 66, 67]; in figure 4(b), it is assumed that the same CR spectrum is composed only of protons. Note that the assumed composition affects both the conventional and prompt atmospheric neutrino fluxes. As in figure 1, two lines are given for the prompt atmospheric neutrino predictions, to indicate the range of uncertainties arising from different prescriptions for the small-x QCD.

3. Conclusions

By focusing on shower events in which there are no distinguishable muon tracks, the background coming from the conventional atmospheric flux is significantly reduced, allowing greater sensitivity to new physics signals, i.e., the prompt atmospheric neutrino flux or a diffuse extragalactic neutrino flux coming from unresolved sources. Considering the shower spectra, the spectral break occurs about an order of magnitude lower in energy than when considering the usual ν_μ charged-current track channel. In addition, in the shower channel there is a much closer relationship between neutrino and visible energy, which will provide better resolution for searching for a spectral break. This technique should be particularly useful for measuring the prompt atmospheric neutrino flux; since it is very steeply falling, it benefits more than an extragalactic neutrino flux from a reduction in the analysis threshold. Although the expected rates, shown in figure 4, are not large, they predict the observation of a sufficient number of events per year, which make feasible the identification of new high energy neutrino signals. It should be also noted that the AMANDA bound [21] allows larger fluxes, up to about two orders of magnitude, which would give much larger rates. Indeed, here we show that the high energy neutrino signals can be observed even in the most pessimistic scenarios assumed for the prompt and extragalactic neutrino fluxes. Even before the prompt atmospheric or extragalactic neutrino fluxes are discovered, this technique would allow a high statistics measurement of the conventional atmospheric neutrino flux, essential for verifying its extrapolation.

Once a break in the spectrum has been observed, several characteristics can be used to distinguish the prompt atmospheric neutrino flux from an extragalactic flux. If there are sufficient events above the break, the spectra should be quite different. In particular, the extragalactic neutrino flux should fall more slowly and will also initiate more high energy muons; the one highest energy event has a powerful lever arm for determining the spectral index [58]. The ν_τ component is small for the prompt atmospheric neutrino flux but large for an extragalactic flux; if any ν_τ charged-current events are individually identified at high energies, then an extragalactic neutrino flux would be indicated [58]. Finally, the identification of point and/or transient extragalactic sources will improve the estimates of the diffuse extragalactic flux due to unresolved sources.

In conclusion, we have shown that the charged-current *electron* neutrino shower channel should be particularly effective for suppressing the conventional atmospheric neutrino background, leading to the robust identification of new physics components of the high energy neutrino flux, either the prompt atmospheric neutrinos, or the diffuse extragalactic neutrino background, or both.

Acknowledgments

References

[1] Cronin J W, 2004 *Preprint* astro-ph/0402487
[2] Harari D, Mollerach S, Roulet E and Sánchez F, 2002 *J. High Energy Phys.* JHEP03(2002)045 [SPIRES]
[3] Dolag K, Grasso D, Springel V and Tkachev I, 2003 *Preprint* astro-ph/0310902
[4] Sigl G, Miniati F and Ensslin T A, 2004 *Preprint* astro-ph/0401084
[5] Kneiske T M, Mannheim K and Hartmann D H, 2002 *Astron. Astrophys.* **386** 1 [SPIRES]
[6] Kneiske T M, Mannheim K and Hartmann D H, 2004 *Astron. Astrophys.* **413** 807 [SPIRES]
[7] Learned J G and Mannheim K, 2000 *Ann. Rev. Nucl. Part. Sci.* **50** 679 [SPIRES]
[8] Albuquerque I F M, Lamoureux J and Smoot G F, 2002 *Astrophys. J. Suppl.* **141** 195
[9] Halzen F and Hooper D, 2002 *Rep. Prog. Phys.* **65** 1025
[10] Spiering C, 2003 *J. Phys. G: Nucl. Part. Phys.* **29** 843 [SPIRES]
[11] Torres D F and Anchordoqui L A, 2004 *Rep. Prog. Phys.* **67** 1663
[12] Aharonian F A *et al*, 1999 *Astron. Astrophys.* **349** 11 [SPIRES]
[13] Krennrich F *et al*, 2001 *Astrophys. J.* **560** L45 [SPIRES]
[14] Krennrich F *et al*, 2002 *Astrophys. J.* **575** L9 [SPIRES]
[15] Aharonian F A *et al*, 2003 *Astron. Astrophys.* **410** 813 [SPIRES]
[16] Andrés E *et al* (AMANDA Collaboration), 2001 *Nature* **410** 441 [SPIRES]
[17] Ahrens J *et al* (AMANDA Collaboration), 2002 *Phys. Rev.* D **66** 012005 [SPIRES]
[18] Ahrens J *et al* (AMANDA Collaboration), 2003 *Phys. Rev. Lett.* **90** 251101 [SPIRES]
[19] Ahrens J *et al* (AMANDA Collaboration), 2003 *Phys. Rev.* D **67** 012003 [SPIRES]
[20] Kowalski M, 2003 *PhD Thesis* Humboldt-University, Berlin http://area51.berkeley.edu/manuscripts/
[21] Ackermann M *et al* (AMANDA Collaboration), 2004 *Preprint* astro-ph/0405218
[22] Ahrens J *et al* (IceCube Collaboration), 2004 *Astropart. Phys.* **20** 507 [SPIRES]
[23] Kajita T and Totsuka Y, 2001 *Rev. Mod. Phys.* **73** 85 [SPIRES]
[24] Gaisser T K and Honda M, 2002 *Ann. Rev. Nucl. Part. Sci.* **52** 153 [SPIRES]
[25] Woschnagg K, 2004 *Talk at Neutrino 2004* http://neutrino2004.in2p3.fr/
[26] Balkanov V *et al* (BAIKAL Collaboration), 2001 *Proc. 9th Int. Symp. on Neutrino Telescopes (Venice)* [astro-ph/0105269]
[27] Balkanov V *et al* (BAIKAL Collaboration), 2002 *Preprint* astro-ph/0211571
[28] Ayutdinov V *et al* (BAIKAL Collaboration), 2003 *Proc. 28th Int. Cosmic Ray Conf. (Tsukuba)* p 1353
[29] Zas E, Halzen F and Vázquez R A, 1993 *Astropart. Phys.* **1** 297 [SPIRES]
[30] Thunman M, Ingelman G and Gondolo P, 1996 *Astropart. Phys.* **5** 309 [SPIRES]
[31] Pasquali L, Reno M H and Sarcevic I, 1998 *Astropart. Phys.* **9** 193 [SPIRES]
[32] Pasquali L, Reno M H and Sarcevic I, 1999 *Phys. Rev.* D **59** 034020 [SPIRES]
[33] Volkova L V and Zatsepin G T, 2001 *Yad. Fiz.* **64** 313 [SPIRES]
    Volkova L V and Zatsepin G T, 2001 *Phys. Atom. Nucl.* **64** 266 [SPIRES] (translation)
[34] Costa C G S, 2001 *Astropart. Phys.* **16** 193 [SPIRES]
[35] Costa C G S, Halzen F and Salles C, 2002 *Phys. Rev.* D **66** 113002 [SPIRES]
[36] Martin A D, Ryskin M G and Staśto A M, 2003 *Acta Phys. Polon.* B **34** 3273
[37] Candia J and Roulet E, 2003 *J. Cosmol. Astropart. Phys.* JCAP09(2003)005 [SPIRES]
[38] Gelmini G, Gondolo P and Varieschi G, 2003 *Phys. Rev.* D **67** 017301 [SPIRES]
[39] Hooper D, Nunokawa H, Peres O L G and Zukanovich Funchal R, 2003 *Phys. Rev.* D **67** 013001 [SPIRES]
[40] Staśto A M, 2004 *Int. J. Mod. Phys.* A **19** 317 [SPIRES]
[41] Waxman E and Bahcall J, 1999 *Phys. Rev.* D **59** 023002 [SPIRES]
[42] Volkova L V, 1980 *Yad. Fiz.* **31** 1510 [SPIRES]
    Volkova L V, 1980 *Sov. J. Nucl. Phys.* **31** 784 [SPIRES] (translation)

[43] Bugaev E V and Naumov V A, 1987 *Yad. Fiz.* **45** 1380 [SPIRES]
  Bugaev E V and Naumov V A, 1987 *Sov. J. Nucl. Phys.* **45** 857 [SPIRES] (translation)
[44] Bugaev E V and Naumov V A, 1989 *Phys. Lett.* B **232** 391 [SPIRES]
[45] Barr G, Gaisser T K and Stanev T, 1989 *Phys. Rev.* D **39** 3532 [SPIRES]
[46] Honda M, Kasahara K, Hidaka K and Midorikawa S, 1990 *Phys. Lett.* B **248** 193 [SPIRES]
[47] Lipari P, 1993 *Astropart. Phys.* **1** 195 [SPIRES]
[48] Honda M, Kajita T, Kasahara K and Midorikawa S, 1995 *Phys. Rev.* D **52** 4985 [SPIRES]
[49] Agrawal V, Gaisser T K, Lipari P and Stanev T, 1996 *Phys. Rev.* D **53** 1314 [SPIRES]
[50] Lipari P, Gaisser T K and Stanev T, 1998 *Phys. Rev.* D **58** 073003 [SPIRES]
[51] Battistoni G, Ferrari A, Lipari P, Montaruli T, Sala P R and Rancati T, 2000 *Astropart. Phys.* **12** 315
    [SPIRES]
[52] Fiorentini G, Naumov V A and Villante F L, 2001 *Phys. Lett.* B **510** 173 [SPIRES]
[53] Barr G, Gaisser T K, Lipari P, Robbins S and Stanev T, 2003 *Phys. Rev.* D **70** 023006 [SPIRES]
[54] Honda M, Kajita T, Kasahara K and Midorikawa S, 2004 *Preprint* astro-ph/0404457
[55] Halzen F and Saltzberg D, 1998 *Phys. Rev. Lett.* **81** 4305 [SPIRES]
[56] Beacom J F, Crotty P and Kolb E W, 2002 *Phys. Rev.* D **66** 021302 [SPIRES]
[57] Dutta S I, Reno M H and Sarcevic I, 2002 *Phys. Rev.* D **66** 077302 [SPIRES]
[58] Beacom J F, Bell N F, Hooper D, Pakvasa S and Weiler T J, 2003 *Phys. Rev.* D **68** 093005 [SPIRES]
[59] Hussain S and McKay D W, 2004 *Phys. Rev.* D **69** 085004 [SPIRES]
[60] Yoshida S, Ishibashi R and Miyamoto H, 2004 *Phys. Rev.* D **69** 103004 [SPIRES]
[61] Bugaev E, Montaruli T, Shlepin Y and Sokalski I, 2004 *Astropart. Phys.* **21** 491 [SPIRES]
[62] Jones J, Mocioiu I, Reno M H and Sarcevic I, 2004 *Phys. Rev.* D **69** 033004 [SPIRES]
[63] Lai H *et al* (CTEQ Collaboration), 1995 *Phys. Rev.* D **51** 4763 [SPIRES]
[64] Golec-Biernat K J and Wüsthoff M, 1999 *Phys. Rev.* D **59** 014017 [SPIRES]
[65] Bartels J, Golec-Biernat K J and Kowalski H, 2002 *Phys. Rev.* D **66** 014001 [SPIRES]
[66] Candia J, Roulet E and Epele L N, 2002 *J. High Energy Phys.* JHEP12(2002)033 [SPIRES]
[67] Candia J, Mollerach S and Roulet E, 2003 *J. Cosmol. Astropart. Phys.* JCAP05(2003)003 [SPIRES]
[68] Beacom J F, Bell N F, Hooper D, Pakvasa S and Weiler T J, 2003 *Phys. Rev. Lett.* **90** 181301 [SPIRES]
[69] Barenboim G and Quigg C, 2003 *Phys. Rev.* D **67** 073024 [SPIRES]
[70] Keranen P, Maalampi J, Myyrylainen M and Riittinen J, 2003 *Phys. Lett.* B **574** 162 [SPIRES]
[71] Beacom J F, Bell N F, Hooper D, Pakvasa S and Weiler T J, 2004 *Phys. Rev.* D **69** 017303 [SPIRES]
[72] Beacom J F, Bell N F, Hooper D, Learned J G, Pakvasa S and Weiler T J, 2004 *Phys. Rev. Lett.* **92** 011101
    [SPIRES]
[73] Gandhi R, Quigg C, Reno M H and Sarcevic I, 1998 *Phys. Rev.* D **58** 093009 [SPIRES]
[74] L'Abbate A, Montaruli T and Sokalski I, 2004 *Preprint* hep-ph/0406133
[75] Stecker F W, 1979 *Astrophys. J.* **228** 919 [SPIRES]
[76] Berezinsky V S, Gaisser T K, Halzen F and Stanev T, 1993 *Astropart. Phys.* **1** 281 [SPIRES]
[77] Domokos G, Elliott B and Kovesi-Domokos S, 1993 *J. Phys. G: Nucl. Part. Phys.* **19** 899 [SPIRES]
[78] Ingelman G and Thunman M, 1996 *Preprint* hep-ph/9604286
[79] Athar H, Cheung K M, Lin G L and Tseng J J, 2003 *Astropart. Phys.* **18** 581 [SPIRES]